Chemical Science

ROYAL SOCIETY OF CHEMISTRY

PERSPECTIVE

View Article Online
View Journal | View Issue

Open Access Article. Published on 16 oajagemánnu 2024. Downloaded on 2026-02-06 10:16:02.
This article is licensed under a Creative Commons Attribution-NonCommercial 3.0 Unported Licence.

Check for updates

Cite this: *Chem. Sci.*, 2024, **15**, 1924

All publication charges for this article have been paid for by the Royal Society of Chemistry

Received 30th October 2023
Accepted 6th December 2023

DOI: 10.1039/d3sc05787a

rsc.li/chemical-science

Porous organic framework membranes based on interface-induced polymerisation: design, synthesis and applications

Lin Liu,†[a] Ruihe Yu,†[a] Liying Yin,[ab] Ning Zhang *[a] and Guangshan Zhu *[a]

Porous organic frameworks (POFs) are novel porous materials that have attracted much attention due to their extraordinary properties, such as high specific surface area, tunable pore size, high stability and ease of functionalisation. However, conventional synthesised POFs are mostly large-sized particles or insoluble powders, which are difficult to recycle and have low mass transfer efficiencies, limiting the development of their cutting-edge applications. Therefore, processing POF materials into membrane structures is of great significance. In recent years, interface engineering strategies have proved to be efficient methods for the formation of POF membranes. In this perspective, recent advances in the use of interfaces to prepare POF membranes are reviewed. The challenges of this strategy and the potential applications of the formed POF membranes are discussed.

1 Introduction

Advanced porous materials have become a research focus of various fields due to the diversity of their building blocks and functionalities.[1] The development of porous materials has gone through traditional porous carbon, zeolite molecular sieves and porous organic frameworks (POFs).[2–4] Among them, POFs are usually classified into the following types based on their structural characteristics: metal organic frameworks (MOFs), covalent organic frameworks (COFs), porous aromatic frameworks (PAFs), covalent triazine frameworks (CTFs), conjugated microporous polymer (CMP), *etc.*[5–8] Compared with inorganic materials, the building blocks of POFs contain organic small molecules with a wide variety of sources, which facilitates the targeted modulation of the structure and function of POFs through the diversity of building units. Due to the advantages of high specific surface area, tunable channels, and excellent stability, POFs have been widely studied and shown excellent application prospects in the fields of gas storage and separation, non-homogeneous catalysis, energy storage materials, sensing, and drug delivery.[9–12]

Early efforts have been devoted to the development of POF structure and functionality, and promising results have been achieved.[13] However, conventionally synthesised POFs are mostly insoluble powders with active sites deeply buried, interparticle boundaries, and poor recyclability, limiting their applications. Therefore, making POF powders into membranes for a broader practical application is highly demanded.[14,15] In the past decade, there have been numerous strategies for the preparation of thin POF membranes.[16] Initially, researchers mostly prepared mixed matrix membranes by blending POF powders with polymers, but the wide distribution of dopant particles made it difficult to regularise the formation of membranes, leading to internal inhomogeneity or even physical defects in the composite membrane.[17,18] Subsequently, the vacuum-assisted filtration method was developed by layer-by-layer stacking of the nanosheets to form membranes, where the formation of discontinuous channels was inevitable if the layers were not tightly linked.[19] Recently, interface polymerisation has become an effective way for the preparation of continuous pure-phase POF membranes. Interface engineering can position the reaction in the desired place to allow the controlled shaping of the POF membranes at the interface, which represents a powerful tool for tailoring the structure and properties of POF membranes.[20–22] To date, there are several pioneering reviews that have well summarised the strategies for the synthesis of POF membranes and their potential applications in different fields.[23,24] Nevertheless, as far as we know, none of them focuses exclusively on interface polymerisation strategies.

In the current perspective, we first present several recent advances in interface engineering for the construction of POF membranes, focusing on a detailed overview of four different interfaces (Fig. 1), namely gas–liquid, gas–solid, liquid–liquid, and liquid–solid, particularly in the last five years. Next, we summarise the potential applications of continuous pure-phase POF membranes in, *e.g.*, gas separation and water treatment, ion transport, biomedical science, and sensors. Finally, we

[a]*Department of Chemistry, Northeast Normal University, Changchun, China. E-mail: zhangn380@nenu.edu.cn; zhugs100@nenu.edu.cn*

[b]*School of Chemistry and Life Science, Changchun University of Technology, Changchun, China*

† These authors contributed equally to this work.

© 2024 The Author(s). Published by the Royal Society of Chemistry

Open Access Article. Published on 16 oajagemánnu 2024. Downloaded on 2026-02-06 10:16:02.
This article is licensed under a Creative Commons Attribution-NonCommercial 3.0 Unported Licence.

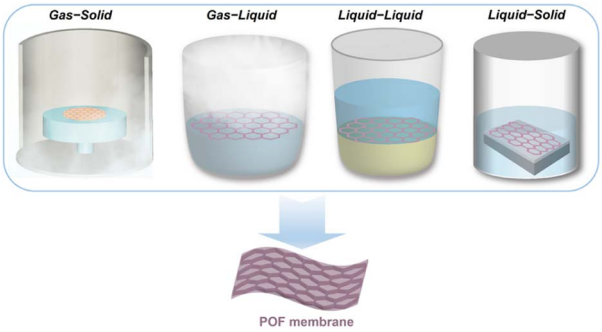

Fig. 1 Schematic illustration of various interfaces involved in the synthesis of functional POF membranes, including gas–solid, gas–liquid, liquid–liquid and liquid–solid interfaces.

provide an outlook on future research directions, and discuss the remaining unresolved challenges, as well as future opportunities. We believe this perspective will not only help to generate more research interest in advanced POF membranes, but also provide implications for interfacial changes in other materials (*e.g.* capsules, nanofibers) and expand the application scope.

2 Most recent advances in the way of synthesising POFs at the interface

2.1 Gas–solid interface

The stable gas–solid interface can confine the reaction to the solid surface by chemical vapour deposition or precursor sublimation, and it can overcome the perturbation effect on the interface caused by temperature increase. Researchers have used the gas–solid interface to build a series of functional thin membrane materials with a variety of structures, compositions and functions.

Wu and Jiang's group reported for the first time the preparation of ultra-thin COF membranes by gas–solid interface polymerisation in 2020 (Fig. 2). By increasing the reaction temperature and optimising the homogeneous distribution of monomers at the solid-phase interface, highly crystalline and ultrathin COF membranes could be obtained in 9 h, which was 8 times shorter than the preparation time of traditional methods, and the thickness of the membrane could be regulated between 20 nm and 1 μm.[25] Although there have been some reports on forming thin membranes on surfaces using vapour deposition, the membrane generally tends to form non-porous phases. The landscape of possible polycrystalline states of some porous materials poses a challenge in controlling the outcome of their synthesis. Researchers used templates to perform controlled growth of zeolite imidazole framework (ZIF) films on the surface with vapor assistance. During the reaction between ZnO and 4,5-dichloroimidazole vapour, the introduction of ethanol or dimethylformamide vapour resulted in the formation of porous ZIF-71, and this approach was equally applicable to other ZIF-series.[26] In order to better explore the structure of the surface COF skeleton as well as the molecular arrangement, Wan and co-workers developed a general method of constructing COF monomolecular layers and films on substrate surfaces based on gas–solid interface reactions. Using this method, it was possible to directly grow COF thin films with large domain area and highly structurally ordered orientation on substrate surfaces with different properties.[27,28] In addition to crystalline COFs and MOFs, POFs also include other materials that have high stability by irreversible coupling reactions such as Ullmann, Sonogashira, and Suzuki. Atomic hydrogen blocks the extent of aryl–aryl bond formation which limits the final size of the materials. First's group synthesised large-sized POF films with an Ullmann-like on-surface reaction by controlling the rate of molecular deposition and substrate temperature in a vacuum environment, and analysed the molecular structure using a scanning tunneling microscope.[29] Moreover, Kawai *et al.* achieved silabenzene-bridged POF materials under ultra-high vacuum conditions using surface synthesis techniques.[30] Besides the use of vacuum-assisted vapour deposition, Schwieger and his colleagues used a versatile and easy spraying process to deposit homogeneous ZnO layers on different carriers, followed by solvent-free conversion of the ZnO layers into dense ZIF-8 membranes by a gas–solid reaction.[31] Notably, neither the structure of ZnO nor the subsequently formed ZIF-8 layer showed any dependence on the support material. This facile approach can be extended to the synthesis of a variety of MOF membranes on different supports.

The gas–solid interface reaction, as a rather novel platform for the preparation of POF thin membranes, can clarify the POF structure from the atomic scale and provide a new research idea for the effective control of the reaction direction. A wide range of reactions can occur at the gas–solid interface, which are particularly suitable for coupling reactions using water–oxygen sensitive catalysts. The monomers are mostly volatile and can be thermally polymerised at the gas–solid interface, and high temperature and high vacuum are normally required to promote the uniform distribution of monomers on the solid surface. However, there are some drawbacks at present, such as the requirement of a harsh environment, and high cost of the reaction process. In addition, transferring monolayer POF membranes from the substrate without damaging the structure is still challenging.

2.2 Gas–liquid interface

Gas–liquid interface polymerisation is an effective way to obtain free-standing independent POF membranes. By polarising the precursor solution, using surfactants, or other ways to confine the reaction at the gas–liquid interface, a flexible POF membrane can be obtained and its size is consistent with the size of the liquid surface.

In 2010, Kitagawa *et al.* constructed 2D-MOF films using the Langmuir–Blodgett (LB) assembly technique for the first time. A solution of 5,10,15,20-tetrakis(4-carboxyphenyl)porphyrinato-cobalt(II) and pyridine dissolved in chloroform/methanol was spread on the surface of an aqueous solution with $CuCl_2 \cdot 2H_2O$ as the subphase, and the thickness of the films was controlled by layer-by-layer stacking.[32] In addition, Feng and Zhang *et al.* have constructed large-area MOF films on the water surface by

Open Access Article. Published on 16 oajagemánnu 2024. Downloaded on 2026-02-06 10:16:02.
This article is licensed under a Creative Commons Attribution-NonCommercial 3.0 Unported Licence.

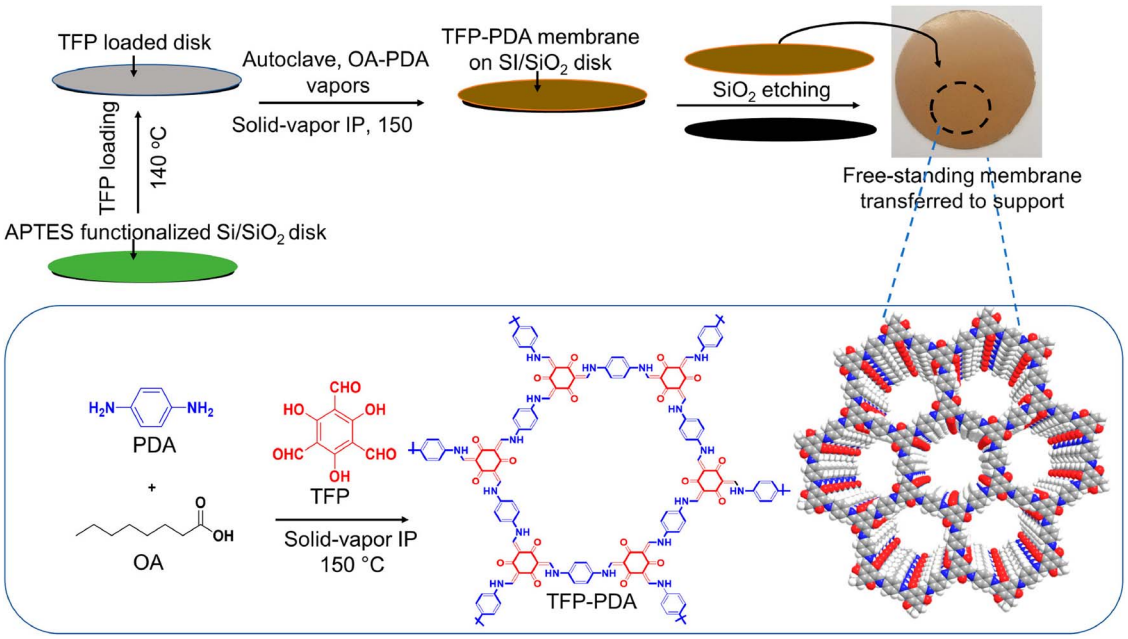

Fig. 2 Scheme of solid–vapor interfacial polymerisation (IP) for the 1,3,5-triformylphloroglucinol-polyamide (TFP-PDA) membrane, including membrane growth and HF etching step to obtain a free-standing membrane. Digital photos of the TFP-PDA membrane and the molecular reaction are presented. Copyright 2020 American Chemical Society.

microwave irradiation. Highly crystalline MOF films could be synthesised in less than three minutes, with lateral dimensions of up to 23 cm^2 (Fig. 3).[38] Subsequently, in 2018, Lai *et al.* introduced the LB method to the preparation of COF membranes and successfully constructed crystalline COF thin membranes using 1,3,5-triformylphloroglucinol and 9,9-dihexylfluorene-2,7-diamine.[33] It was the first attempt to synthesise large-area 2D COF membranes using the LB method, which

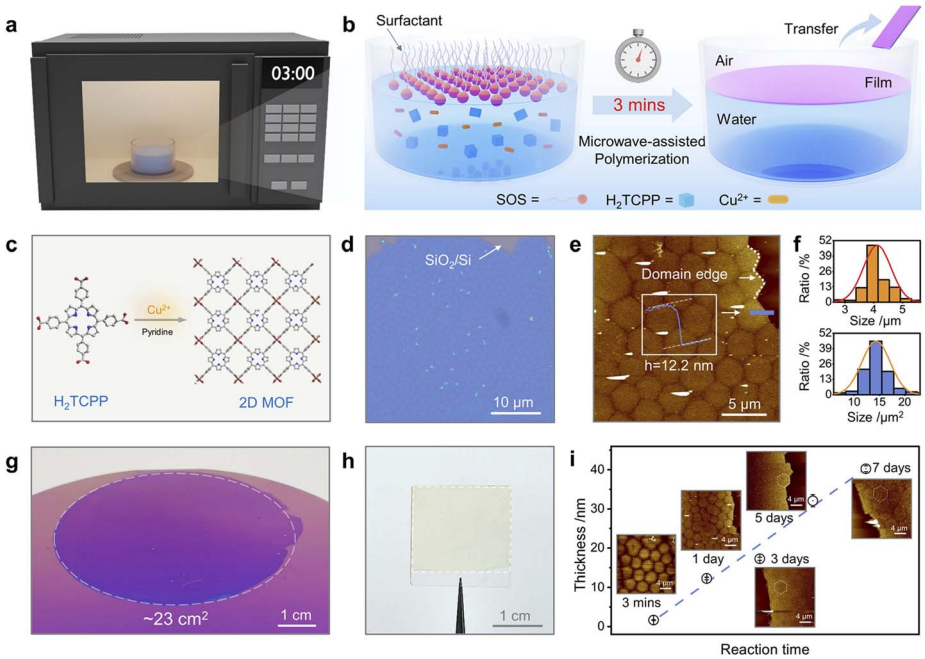

Fig. 3 Synthesis and morphology of 2D MOF thin film. (a) Illustration of the microwave oven. (b) Synthesis of a 2D MOF on the water surface. (c) Chemical structures of monomer and 2D MOF. (d) Optical microscopy image of 2D MOF after 24 h polymerisation. (e) AFM image of 2D MOF after 24 h polymerisation. (f) Statistical distribution of the domain size of the 2D MOF crystals. (g) 2D MOF film on a 300 nm SiO_2/Si wafer (diameter Ø = 10 cm). (h) Optical microscopy image of the 2D MOF on quartz. (i) Thickness of 2D MOF *vs.* reaction time (inset: AFM image of the 2D MOF from 3 min to 7 days). Copyright 2023 American Chemical Society.

 © 2024 The Author(s). Published by the Royal Society of Chemistry

Open Access Article. Published on 16 oajagemánnu 2024. Downloaded on 2026-02-06 10:16:02.
This article is licensed under a Creative Commons Attribution-NonCommercial 3.0 Unported Licence.

broadened the scope of application of this technique. In 2015, Bao *et al.* demonstrated the synthesis and device integration of processable in-plane conjugated 2D polymers. After pre-reacting bisaldehyde and trisamine for 24 h and filtering the precipitate, Petri dishes containing the filtered supernatant were reacted in saturated H_2O atmosphere for 2 days, producing a highly reflective red film at the solution/air interface.[34] Feng's group has efficiently synthesised large-sized polyimide and polyaniline films at the air–liquid interface with the assistance of a surfactant monolayer, based on which, they have extended the surfactant-monolayer-assisted interfacial synthesis (SMAIS) method, in which a surfactant monolayer was pre-constructed on the water surface to induce the self-organisation of the reactive precursor at the surfactant/water interface and subsequent two-dimensional polymerisation.[35,36] In this way, three polyimide films with different configurations and pore sizes were synthesised, all of which exhibited high crystallinity, demonstrating the universality of the SMAIS method for the synthesis of highly crystalline dibasic polymer films.[37] In 2022, Zheng *et al.* further proposed a general strategy for creating 2D crystals of COF on water with the help of charged polymers.[39] CTFs with aromatic triazine bonds are a subclass of POFs, and obtaining CTFs under mild conditions is a great challenge due to the high energy barrier of the aromatic nitrile trimerisation reaction. Tan's group prepared free-standing semi-crystalline CTF films with large lateral dimensions and controllable thicknesses by aliphatic amine-assisted interfacial polymerisation. In this case, DMSO soluble aldehyde monomers were converted to DMSO insoluble imine precursors by reaction with hexylamine. The imine precursor could diffuse on the DMSO surface, directing the initial alignment of the aldehyde monomer while generating the DMSO/air interface. In this way, the polymerisation reaction was confined to the interface rather than a homogeneous reaction.[40] The air/organic solvent interfacial polymerisation strategy proposed by the authors addresses the drawback of insufficient monomer solubility in previously reported interfacial strategies and provided ideas for improving the processability of CTF films. Fang *et al.* established a method for the fabrication of large-area, defect-free, free-standing, thickness-adjustable metalloporphyrin-based flexible COF films prepared by domain-limited dynamic polymerisation at the gas–liquid interface. Using this method, the prepared film could be scaled up to 3000 cm^2, and the obtained membrane is tough, free-standing, and strong enough to receive or suspend a certain mass of weights. The thickness of the membranes can be adjusted over a wide range (27–110 nm), and the surface roughness is only around 1.5 nm.[41] Moreover, in 2021, Cuniberti *et al.* investigated by means of a multiscale modelling strategy that dimethylmethylene-bridged triphenylamine building blocks were confined to the air–water interface to form monolayers of COF membranes, and this work provided an important basis for the polymerisation of POF thin membranes at the air–liquid interface.[42] Similarly, Wang *et al.* prepared large-area proton-conducting COF membranes on the surface of liquid water with the assistance of water vapour, and water acted as both a diluent and a structure-directing agent in the reaction system.[43] The strategy using water/water vapour as a unique green additive is worthwhile.

Large-size POF membranes can be formed by continuous supply of reaction basic units and systematic aggregation at the gas–liquid interface. Limiting the reaction to the gas–liquid interface overcomes the problem of self-aggregation in conventional polymerisation reactions. Thus, reactions traditionally occur at high-temperature; gas–liquid interface polymerisation can be carried out at room temperature. It is particularly important to choose the solvent, the higher the solubility of monomers and oligomers in solution, the easier it is to form a dense membrane without defects. However, for water–oxygen-sensitive irreversible coupling reactions, synthesis of POF membranes using gas–liquid interfaces has been rarely reported, which needs to be continuously paid attention to and explored.

2.3 Liquid–liquid interface

A liquid–liquid interface is widely used in the preparation of POF membranes, which can effectively prepare large-area membranes. One general method is to disperse the monomers in two immiscible solvents and form the membrane at the interface of solvents.[44,45] The other method is to disperse the monomer and catalyst in two immiscible solvents.[46–48]

In 2011, De Vos and co-workers used the liquid–liquid interface between immiscible liquids as a template for the preparation of homogeneous MOF layers for the first time.[49] The two-phase mixtures were obtained by replacing the ethanol used in the classical synthesis process with a long-chain alcohol such as 1-octanol. In addition, these membrane layers could form hollow capsules of the MOF material $[Cu_3(BTC)_2]$, exhibiting selective permeability. Jiang *et al.* explored a novel defect engineering strategy to fabricate COF membranes.[50] With the spontaneous diffusion of dialdehyde and monoaldehyde monomers from their respective oil phases into the intermediate aqueous phase, the polymerisation–crystallisation process of the oil–water–oil three-phase synthesis system was catalysed by acetic acid. During the assembly process, an abundance of amino groups was generated *in situ* on the COF nanosheets by constructing missing-linker defects on the imine-linked framework. By modulating the ratio of mixed aldehydes, the amount of amino groups can be precisely controlled. In 2018, Hao *et al.* synthesised free-standing 2D COF films at the oil/water/hydrogel interface by loading two monomers into oil and hydrogel, respectively. This strategy can be extended to the preparation of flexible films of POFs, and it is easy to further tune the monomers, catalysts, and other parameters due to the wide availability of gel materials.[51] Chung *et al.* constructed flexible self-standing pure COF films *via* the liquid–liquid interface at room temperature and atmospheric pressure. The pore size and channel chemistry of COF films can be designed by bridging various molecular building blocks *via* strong covalent bonds.[52] In 2022, they further reported a strategy for the rapid *in situ* growth of thin COF films on cross-linked polyimide substrates. A tris(4-aminophenyl)amine aqueous solution and a benzene-1,3,5-tricarboxaldehyde organic solution were used

Open Access Article. Published on 16 oajagemánnu 2024. Downloaded on 2026-02-06 10:16:02.
This article is licensed under a Creative Commons Attribution-NonCommercial 3.0 Unported Licence.

to form COF composite films by unidirectional diffusion and convection processes.[53] In addition to COF films, Chung *et al.* polymerised cyclodextrin (CD) and trimesoyl chloride (TMC) at the interface to obtain porous films. The CD/TMC nanofilms had both hydrophobic inner cavities and hydrophilic channels. This unique pore structure broadly extends the range of applications.[54] In 2018, Wang *et al.* used interfacial polymerisation to prepare four flexible COF films with different alkoxy side chains. Varying the alkoxy chain length had a great influence on the interfacial polymerisation rate, underlying structures, Young's modulus and other properties of the COF films.[55] Li *et al.* synthesised for the first time two types of C–C bonded 2D-conjugated COF membranes at the water–toluene interface by combining Suzuki polymerisation with interfacial polymerisation. One was porous graphene and the other was a porphyrin-containing 2D-COF.[56] Recently, Giri *et al.* achieved the first directional transformation of organoimine cages into COF film at the liquid–liquid interface under ambient conditions of atmospheric pressure and room temperature (Fig. 4).[57] The unfolding of the cage due to the exchange of imine bonds with aromatic amines led to the generation of imine intermediates. The authors dissolved the imine cage (C1) in chloroform and introduced water as a spacer. The aromatic diamine or triamine linker was dissolved in an aqueous acetic acid solution and added to the top of the aqueous layer. The films obtained by this method had good crystallinity and high porosity (1790 ± 80 m^2 g^{-1}). The COF films had unique nanostructured shapes, and the thicknesses of the different COF films were in the range of 800 nm to 5 μm. The strategy provided by this latest study creates a bridge between 0D-porous organic cages and 2D-porous polymer frameworks, enabling structural transitions between two crystalline entities of different dimensions. In addition, our research group designed and synthesised an ultra-thin PAF membrane with tetra-(4-aminophenyl) porphyrin and trimesoyl chloride on a liquid–liquid interface, which broadened the types of interfacial polymerisation reactions.[58]

In contrast to the temperature used in the synthesis of most bulk COF powders, liquid–liquid interface synthesis reaction systems generally need to be conducted at room temperature or lower to maintain a stable interface. The formed interface acts as a template and provides a 2D-limited interface for the polymerisation reaction. Through various supramolecular interactions between monomers and with solvent molecules, free-standing POF membranes of varying thicknesses from monolayers to micrometres can be obtained which can be simply transferred to any functional substrates for cutting-edge applications. Liquid–liquid interfacial polymerisation is controlled by the chemical kinetics of the monomer contacting directly at the interface. The whole polymerisation process needs to be controlled by the diffusion of monomers through the membrane at the interface. As the membrane thickness increases, the monomer diffusion barrier increases, resulting in slower polymerisation. Simultaneously, the roughness on both sides of the membrane is hard to control, which is unfavourable for subsequent applications. In addition, liquid–liquid interfacial polymerisation is mostly applicable to reversible polycondensation reactions between two or more monomers.

2.4 Liquid–solid interface

The liquid–solid interface strategy is one of the most popular and efficient methods for the preparation of POF membranes. The dimensions of POF membranes obtained on liquid–solid interface depend on the solid-phase substrate. The synthesis of COF films on a liquid–solid interface was first reported by Dichtel's group in 2011.[59] Since then, various substrates have been introduced for different applications. The common method is to immerse the substrate or modified substrate directly into the solution of the POF precursor, and the film is

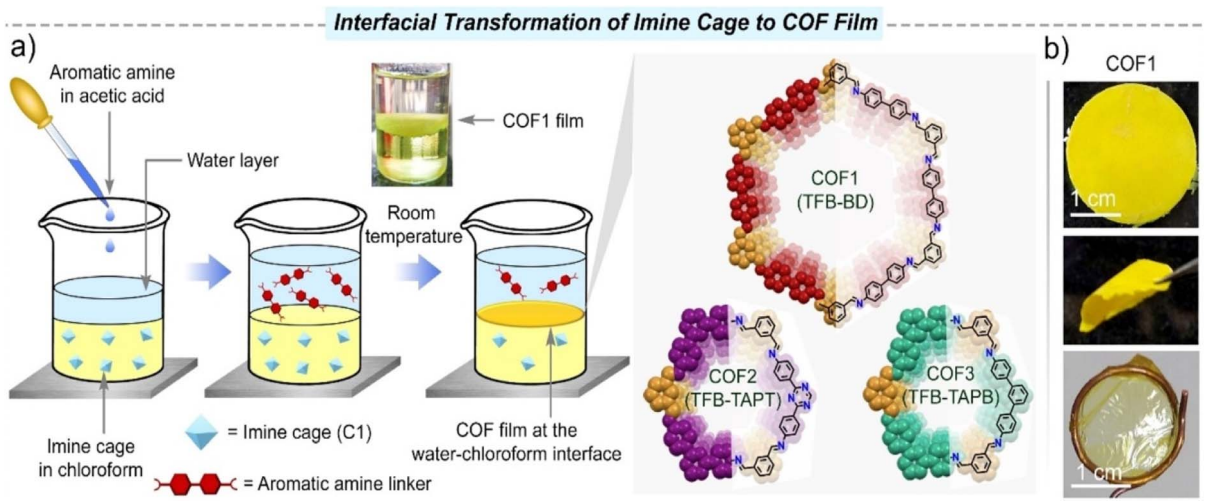

Fig. 4 (a) Representation depicting the acid-catalysed room temperature interfacial transformation of the imine cage into COF film in the presence of diverse amine linkers. The space-filled model of COF1 (TFB-BD), COF2 (TFB-TAPT), and COF3 (TFB-TAPB). The aromatic amines employed for the construction of the respective COF films: COF1: benzidine (BD); COF2: 1,3,5-tris(4-aminophenyl)triazine (TAPT), and COF3: 1,3,5-tris(4-aminophenyl)benzene (TAPB). (b) Digital photographs of COF1 films: free-standing film after 24 h of interfacial polymerisation (top and middle) and solvent-induced delaminated transparent thin film (bottom). Copyright 2023 Wiley-VCH GmbH.

 © 2024 The Author(s). Published by the Royal Society of Chemistry

Open Access Article. Published on 16 oajagemánnu 2024. Downloaded on 2026-02-06 10:16:02.
This article is licensed under a Creative Commons Attribution-NonCommercial 3.0 Unported Licence.

deposited on the surface of the substrate during the reaction process.

In particular, electropolymerisation is one of the powerful tools for the preparation of electroactive and conductive POF membranes on the liquid–solid interface.[60] Gu *et al.* reported the first preparation of CMP films on the liquid–solid interface by the electropolymerisation strategy.[61] Lai's group prepared flexible ionic CMP membranes with a precisely tailored pore structure and chemical properties by a coelectropolymerisation strategy.[62] Our group used electropolymerisation to synthesise PAF films containing carbazole groups on the surface of indium-tinoxide (ITO) glass, which solved the problem of poor film formation caused by the insolubility of conventional PAF powders, and used the PAF materials as a hole-transport layer to produce inverted perovskite solar cells, which could broaden the scope of application of PAF materials.[63]

Surface-initiated polymerisation (SIP) is an important method for surface modification and obtaining polymer coatings.[64] In 2018, Tang *et al.* prepared CMP membranes with high structural rigidity and microporosity at the liquid–solid interface by the SIP strategy.[65] CMP membranes were prepared by solvent-thermal polymerisation of monomers on bromobenzene-modified Si/SiO_2 surfaces, which could be transferred to other porous carriers. Our group has obtained sulfonic COF (SCOF) membranes by the SIP reaction of 1,3,5-triformylphloroglucinol (Tp) and 2,5-diaminobenzenesulfonic acid (Pa-SO_3H) synthesised at the liquid–solid interface (Fig. 5).[66] By controlling the polymerisation time, the thickness of the COF layer could be fine-tuned from 10 to 100 nm. Moreover, free-standing COF membranes could be easily obtained by sacrificing the bridging layer without any decomposition of the COF structure. Subsequently, we also obtained the zwitterionic COF membrane on the Si/SiO_2 surface through SIP.[67] These results show the universality of SIP.

ZIFs are a class of MOF materials with promising applications in molecular separation, pattern formation and sensing.[68–71] However, achieving two-dimensional ZIF crystallisation and ultrathin amorphous ZIF films has been a challenge in the industry, with existing technological approaches producing ZIF films with a thickness of more than 50 nm. Recently, Liu *et al.* synthesised large-area ultrathin and highly oriented ZIF films for the first time, up to the thickness of a single crystal cell, and achieved controllable adjustment of ZIF film thickness.[72] The authors synthesised ZIF films by immersing a number of different substrates into an ultra-dilute precursor solution for a few minutes. The ultra-dilute solution was used here to inhibit uniform nucleation in the native solution. As the number of nuclei in the native solution decreases, the attachment of pre-formed nuclei to the substrate could be reduced or eliminated. The method reported in this work can be extended to other promising MOFs, providing new ideas for constructing novel ultrathin highly oriented MOF films, which are expected to advance the limits of nanoscale patterning. Conjugated monolayer two-dimensional COFs have unique properties with potential applications in sensing, optoelectronics and photonics. Hecht's group has obtained the first vinyl-linked monolayer 2D COF membranes by surface polymerisation using reversible Knoevenagel polycondensation.[73] Self-assembly of two monomers at the liquid/solid interface led to the formation of extended covalent networks at room temperature without the requirement of additional catalysts or reagents. This method enables the formation of extended conjugated 2D polymers under mild conditions.

For the liquid–solid interfacial strategy, self-assembled monolayers (SAMs) and polymer brushes have been typically used as templates for the growth of POFs.[74] Börjesson *et al.* prepared PAF films on a gold substrate *via* the reaction of SAMs with monomers, which led to the growth of smooth and continuous PAF films with a controlled thickness.[75] In 2017, our group used the polymer-anchored surface of silicon wafers to induce the synthesis of MOFs.[76] Most recently, we reported the

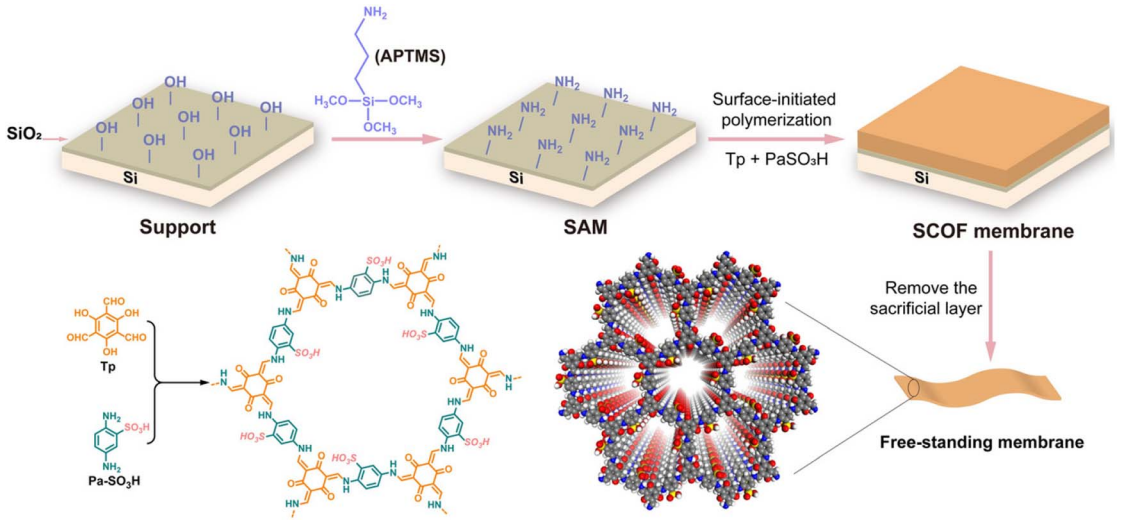

Fig. 5 Schematic route for the preparation of the SCOF membrane grafted on silicon wafers and the free-standing SCOF membrane, molecular structures of Tp, Pa-SO_3H and TpPa-SO_3H. Copyright 2021 Wiley-VCH GmbH.

Open Access Article. Published on 16 oajagemánnu 2024. Downloaded on 2026-02-06 10:16:02.
This article is licensed under a Creative Commons Attribution-NonCommercial 3.0 Unported Licence.

growth of PAFs on the surface of polymer brushes (Fig. 6).[77] In contrast to PAFs formed in solution, polymer brushes provide a confined environment for PAF growth, resulting in nanosized and homogeneous spherical PAFs formed amongst the polymer brushes. The size of PAFs could be tailored from 30 to 500 nm by subtly changing the structural parameters. Poly(styrene)/PAF-1 (PS/PAF-1) porous membrane could be obtained *via* the removal of the SiO_2 layer. Polymer membranes can also be used as reaction substrates. Dai *et al.* obtained hypercross-linked porous polymer (HCP) membranes by *in situ* polymerisation on PS membranes based on Friedel–Crafts reaction.[78]

The liquid–solid interface provides a restricted space between the reactant solution and the substrate surface, and the choice of substrate and template is flexible. A wide variety of POF membranes have been successfully prepared on various functional substrates for cutting-edge applications. During liquid–solid polymerisation, monomer concentration and reactant activity are key factors that affect the quality of the membrane. Lower monomer concentrations inhibit the reaction occurring in the bulk phase and confine the reaction to the surface. Higher reactivity of the reactants leads to faster formation of a dense initial barrier layer. SAMs and polymer brushes as templates for POF growth in liquid–solid interfacial strategies are intriguing and worth exploring in the future.

Multiple POF membranes can be synthesised at each interface type. Specific properties may be different depending on the exact conditions and materials used in each case. For a clear understanding, we summarise the applicability and limitations of the four interface-induced polymerisation strategies in Table 1.

3 Applications of POF membranes

3.1 Gas separation and water treatment

POFs are promising materials for advanced molecular separation membranes. The interface approach enables the construction of continuous, defect-free, pure-phase POF thin membranes. Since the pore size of POF is much larger than most gas and ion sizes, it is necessary to reduce the pore size to the microporous range, effective and uniform molecular channels are formed. At the same time, the molecular adsorption is promoted through the coordinated regulation of the pore structure, which can further realise the efficient separation of gas or liquid mixture.[79]

Our group synthesised the first continuous cationic PAF membrane (iPAF-5) on the surface of silicon wafers with gas separation performance and realised the modulation of the pore size as well as the chemical properties of PAF membranes. The PAF membranes exhibited excellent gas separation performance for different gas mixtures, such as H_2/N_2, CO_2/N_2, *etc.* (Fig. 7).[80] iPAF-5(Cl) had a high gas permeability due to its large pore size (0.76 nm), but poor sieving ability for different gases. When Br^- or BF_4^- was used to replace Cl^-, the pore size of iPAF-5(Br) and iPAF-5(BF_4) was adjusted to 0.48 nm, which realized the precise modulation of the pore size at the molecular level. For H_2/N_2, it showed that all three iPAF-5 continuous membranes exceeded the Robeson upper bound (Fig. 7c). Although the pore sizes of iPAF-5(Br) and iPAF-5(BF_4) are comparable, iPAF-5(Br) has a stronger binding ability to CO_2 molecules than iPAF-5(BF_4). The diffusion of CO_2 within the membrane of iPAF-5(Br) was inhibited, and the transport of CO_2 was greatly slowed down. As shown in Fig. 7d, only iPAF-5(BF_4)'s plot reached the upper side of the bound. Although the membrane showed an optimised CO_2 permeance of 23 058 GPU (gas permeation units), the CO_2/N_2 selectivity of 60 is still lower than that of polymer-based transport membranes, *e.g.*, the interface self-assembly of poly(vinylamine) and polymer-modified MOF has a CO_2/N_2 mixed gas selectivity of 242.[81] Therefore, the goal is to increase the selectivity while maintaining a high level of permeance.

Fan and his co-workers used SIP to synthesise a series of bilayer membranes on the surface of Al_{2O3} substrate (*e.g.* MOF in COF, COF–COF) to form a special interlaced network of micro/nanopores.[82,83] Among them, the COF–COF bilayer membrane demonstrated excellent molecular sieving performance for the separation of H_2/CO_2, H_2/N_2, and H_2/CH_4

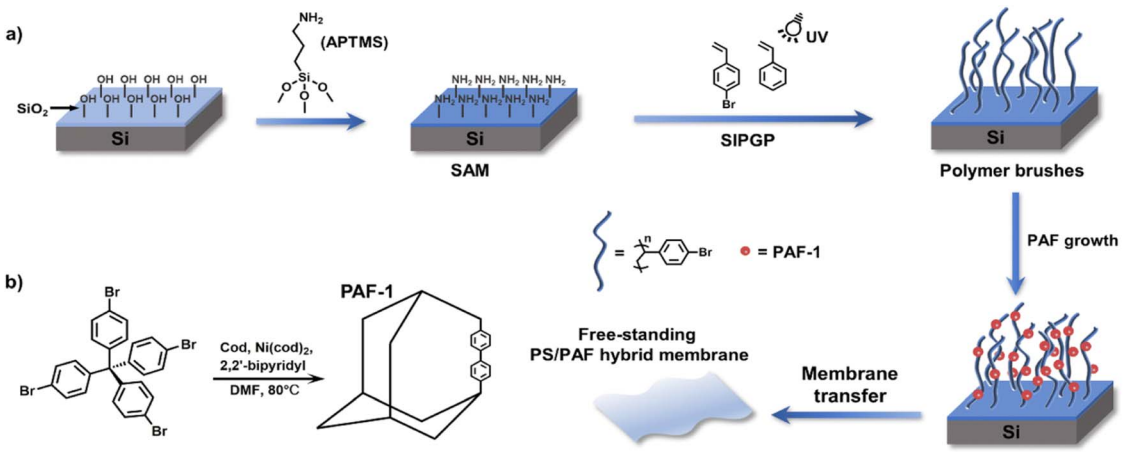

Fig. 6 (a) Scheme for the preparation of PS-Br brushes grafted on silicon substrates, the subsequent PAF growth on the surface, and the fabrication of a hybrid membrane; (b) the synthetic routine for PAF-1. Copyright 2023 Royal Society of Chemistry.

 © 2024 The Author(s). Published by the Royal Society of Chemistry

Open Access Article. Published on 16 oajagemánnu 2024. Downloaded on 2026-02-06 10:16:02.
This article is licensed under a Creative Commons Attribution-NonCommercial 3.0 Unported Licence.

Table 1 The applicability, merits and demerits of interface-induced polymerisation employed in the membrane formation

Interface type	Bonding	POFs	Merits	Demerits
Gas–solid	C–N			
	C=N	COF	Defined structure	Harsh environment
	C–C	PAF	Suitable for water–oxygen sensitive reactions	High cost
	Si–Br	MOF		Hard to transfer
	Coordination bond			
Gas–liquid	C–N	COF		
	C=N	CTF	Large-size preparation	Not suitable for water–oxygen sensitive reactions
	Triazine	Polyimide	Membrane is easy to transfer	
	CO–NH	Polyamide		
	Coordination bond			
Liquid–liquid	C–N			
	C=N	COF	Room temperature synthesis	Monomer diffusion blocked
	C–C	PAF	Membrane is easy to transfer	Long reaction time
	CO–NH	CD/TMC		
	CO–O	MOF		
	Coordination bond			
Liquid–solid	C–N	COF	Flexible choice of substrates and templates	Difficult for mass production
	C=N	CMP		
	C=C	PAF		
	C≡C	HCP		
	C–C	MOF		
	Coordination bond			

mixtures, which far exceeded the Robeson upper bound. The MOF-in-COF membrane similarly exhibited excellent hydrogen permeability (>3000 GPU) and significantly improved the separation selectivity of hydrogen to other gases. In 2023, they embedded tubular-structured α-cyclodextrins into COF pores by means of host–guest encapsulation and prepared ultra-microporous COF membranes with a hierarchical structure by *in situ* interfacial polymerisation to achieve H_2 permeability and high selectivity in gas mixtures.[84] In 2022, Zhao *et al.* have also prepared COF–COF multilayer membranes with an interfacial engineering strategy for gas separation. The COF-LZU1 film with a large pore size was synthesised at the interface, followed by the layer-by-layer interfacial growth of TpTGCl@TpPa-SO_3H to form the COF multilayer membrane with a narrow pore size. The membranes had a high H_2 transmittance of 2163 GPU and H_2/CO_2 selectivity of 26.[85]

In addition to gas separation, POF membranes have potential applications in water treatment. In 2020, Ma *et al.* used

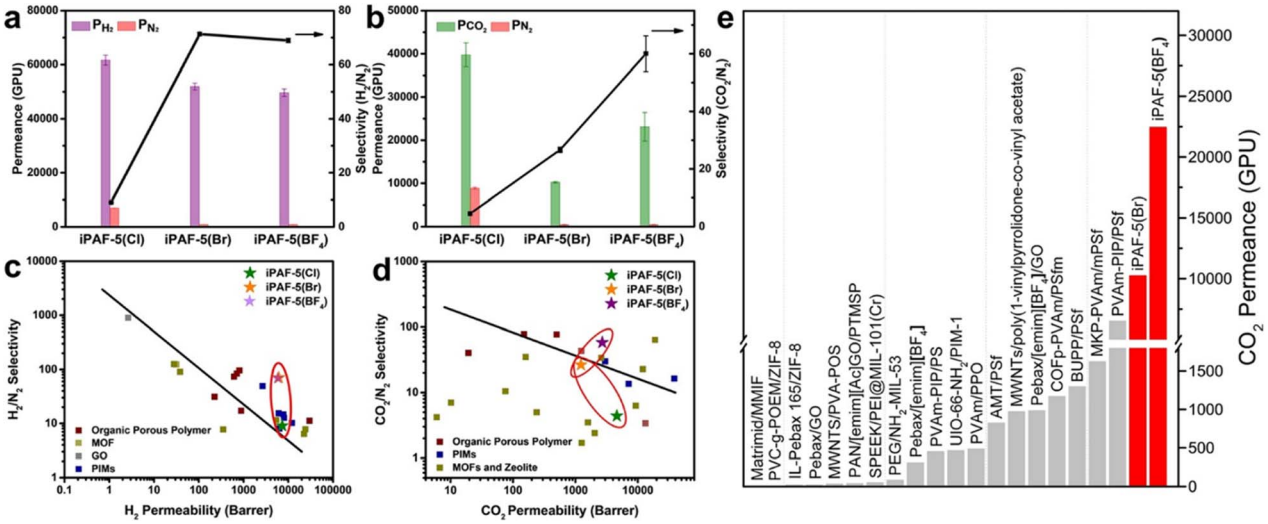

Fig. 7 (a) Permeance and selectivity of continuous PAF membranes for the binary H_2/N_2 mixture. (b) Permeance and selectivity of continuous PAF membranes for the binary CO_2/N_2 mixture. (c) Comparison of the H_2/N_2 separation performance of continuous PAF membranes with other state-of-the-art continuous microporous membranes in Robeson's plots. Square symbols: color coded for different materials in earlier work; Star symbols: PAF membranes in the present work. (d) Comparison of the CO_2/N_2 separation performance of continuous PAF membranes with other state-of-the-art continuous microporous membranes in the corresponding Robeson's plots. (e) Comparison of the CO_2 permeance in gas permeation unit for the iPAF-5(BF_4) membrane with other mixed-matrix membranes. Copyright 2021 Wiley-VCH GmbH.

Open Access Article. Published on 16 oajagemánnu 2024. Downloaded on 2026-02-06 10:16:02.
This article is licensed under a Creative Commons Attribution-NonCommercial 3.0 Unported Licence.

liquid–liquid interfacial polymerisation to form large-size COF membranes, and changed the stacking of the COF layers to achieve COF pore sizes at the sub-nm level. COF membranes had higher ion/molecule rejection and better water permeability, which is potentially valuable in water treatment and gas separation.[86] Jiang *et al.* prepared COF thin membranes with high crystallinity and no defects by using the "liquid–gas phase switching method". The regular one-dimensional through-channel gave the membrane ultra-high solvent permeability (water ~403 L m^{-2} bar^{-1} h^{-1}, acetonitrile ~519 L m^{-2} bar^{-1} h^{-1}) and excellent retention of organic molecules (>98% for a wide range of organic small molecule dyes).[87] Our group prepared COF membranes with tunable thickness using the screen printing technique for the first time. Due to its suitably sized hydrophilic pores, the membrane had high water permeability and can be used for water desalination.[88]

Researchers have mostly achieved the reduction of POF pore size through staggered stacking, directional growth, and hybridisation with other ultra-microporous materials to improve the molecular sieving effect, but precisely regulating the sub-nanometer scale pore size is still a major challenge.

3.2 Ion transport

POFs are considered as promising candidates for ionic and proton conductive membranes because of their sequential transport channels, designable structure and tailored functionality. POF membranes obtained by interface polymerisation possess ultra-high conductivity, and have shown potential in related application fields.

Biological cell membranes are capable of efficient and selective ion transport, but it is more difficult to achieve similar functions in artificial membranes. Lai's group reported a highly crystalline amino-COF membrane, which acted as ion-selective switches to manipulate Na^+ and K^+ transport.[89] The membranes were prepared using interfacial synthesis by *in situ* growth on a polyacrylonitrile (PAN) ultrafiltration membrane carrier. By controlling the influx of Na^+ and efflux of K^+, the authors were able to switch the polarity of the membrane between positive and negative states, which was analogous to the reversal of membrane potential during neural signal transduction *in vivo*.

Sun *et al.* demonstrated the use of COF-based ion-selective membranes to derive energy from low-grade heat sources and the inherent Gibbs free energy of fluid systems (Fig. 8).[90] The membranes were prepared by dissolving diamine compounds and Tp in aqueous acetic acid and toluene to produce aqueous and organic phases, respectively, which were transferred into vessels having two chambers separated by a PAN ultrafiltration membrane. The authors demonstrated that higher charge quantity conductance resulted in lower impediments to ion transport across the membrane, with a maximum output power density of 97 W m^{-2}, which was approximately 20 times that of the commercial benchmark. The power value could be further increased by applying a temperature gradient to 231 W m^{-2}. Besides, due to the presence of intrinsically interconnected nano-channels, 3D-COF emerged as a promising candidate for next-generation proton conducting materials in redox flow batteries, electrochemical sensors, and fuel cells.[91] Jiang *et al.* prepared freestanding homogeneous 3D COF-300 membranes using a liquid–liquid interfacial polymerisation strategy.[92] In addition, by encapsulating etidronic acid as a proton carrier in the nanochannels of COF-300 membranes, etidronic acid@COF-300 membranes were prepared, achieving a proton conductivity of 0.650 S cm^{-1} at 90 °C.

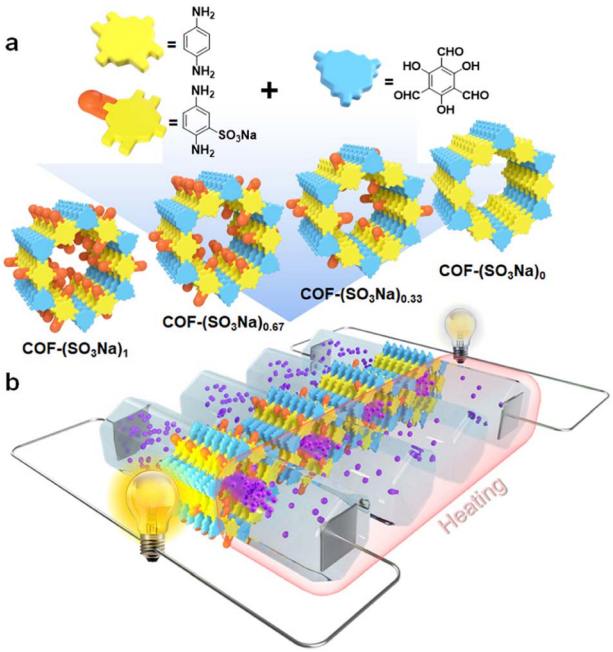

Fig. 8 (a) Synthetic scheme of ionic COF membranes with varied charge density and (b) conceptual illustration of the conversion of energies derived from low-grade heat and salinity differences into electricity using ionic COF membranes, and the impact of the membrane charge density on the output power density. Copyright 2022 Wiley-VCH GmbH.

Wang *et al.* prepared sp^2 carbon-conjugated COFs (sp^2c-COFs) on various solid substrates (*e.g.* fluorine-doped tin oxide, aluminium sheets, polyacrylonitrile films) *via* self-assembly monolayer-assisted surface-initiated Schiff-base-mediated aldol polycondensation, yielding large-area, self-supported and crystalline sp^2c-COFs.[93] The authors showed that the COF films with nitrogen-enriched and quasi-1D channels provided excellent anion selectivity. An sp^2c-COF film osmotic power generation device had an output power density of 14.1 W m^{-2} under harsh conditions, which exceeded most reported COF films as well as the commercially available benchmark device (5 W m^{-2}).

POFs with electronic conductivity comparable to metals can advance the fields of organic electronics, catalysis and energy storage. However, low conductivity limits their practical applications. The development of POF membranes with high electronic conductivity will be a continuing hot topic for the membrane community in the future.

3.3 Biomedical science

POF membranes have received great attention in biomedical applications due to their variable elemental composition and

 © 2024 The Author(s). Published by the Royal Society of Chemistry

Open Access Article. Published on 16 oajagemánnu 2024. Downloaded on 2026-02-06 10:16:02.
This article is licensed under a Creative Commons Attribution-NonCommercial 3.0 Unported Licence.

ordered structure. They have shown promise in biomedical fields such as phototherapy, drug delivery and combination therapy.

Liao *et al.* proposed a strategy to expand the separation surface area of nanofiltration membranes by grafting highly porous porphyrin–aniline CMP (PACMP) on polyamide.[94] The CMP–polyamide composite membranes were formed by one-step interfacial polymerisation to produce ultra-permeable membranes (61.8 L m^{-2} h^{-1}) with a salt (Na_2SO_4) interception above 91.6%. Moreover, due to the generation of reactive oxygen species from the porphyrin moiety of PACMPs, the photoexcited singlet oxygen ($^1O_2$) generated *in situ* could kill 98.5% of *E. coli* and 99.7% of *S. aureus*, which resulted in the excellent antimicrobial performance of the CMP–polyamide composite membrane.

The capability to control the release of small drugs is crucial in biomedicine. Tang's group prepared biocompatible COF membranes by an interfacial polymerisation strategy.[95] The prepared membranes could be easily combined with polymer membranes and integrated into homemade diffusion devices for drug release measurements. The release of organic molecules (*e.g.*, small organic dyes and peptides) through COF membranes with ordered nanoscale pores was investigated, showing a constant zero-grade release behaviour. Meanwhile, biological evaluations showed that the COF membrane-based release system was biocompatible and the COF membrane exhibited high stability for long-term release of small molecules in aqueous media. Dong *et al.* reported a porphyrin–COF-based membrane encapsulating ibuprofen (IBU) by interfacial polymerisation *in situ* and impregnation (Fig. 9).[96] The obtained IBU@DhaTph [Dha: 2,5-dihydroxyterephthalaldehyde; Tph: 5,10,15,20-tetrakis (4-aminophenyl) porphyrin] membranes exhibited efficient antimicrobial and anti-inflammatory effects *via* synergistic photo-induced $^1O_2$, generation and controlled IBU release, which were well supported by experiments *in vitro*. Furthermore, biocompatible "band-aid" type dressings based on IBU membranes were prepared, and their excellent anti-infective and tissue remodelling activities were proved by chronic wound healing experiments *in vivo*.

Zhou *et al.* generated porous COF films on ITO *in situ*.[97] An effective photoelectrochemical (PEC) burst probe was designed by loading a large number of $AgInS_2$ quantum dots on gold nanoparticles. After targeting an HIV-induced cyclic amplification process to generate abundant DNA S0, the Au nanoparticles-$AgInS_2$ quantum dot probe was bound to the COF films by DNA hybridisation, which caused the PEC signal of the COF film to be "switched off" for the ultrasensitive detection of HIV. This work opens up a unique two-dimensional COF film-based PEC biosensing platform with good signals for rapid dual-target detection, which can effectively avoid false-positives and false-negatives and shows promising applications in the early prevention and detection of cancer diseases. Homocysteine (Hcy) is a metabolite in the human body and an important determinant of cardiovascular health. Recently, a laser desorption/ionisation mass spectrometry (LDI-MS) method based on COF films was developed for the rapid and sensitive determination of Hcy in human serum using isotopically labelled internal standards by Lin *et al.*[98] The author cultivated COFs on an ITO substrate at room temperature to form a thin film, which was used in LDI-MS. The use of COF film as a substrate with high signal intensity and clean background helped to analyse a range of small molecules such as amino acids, bisphenols, oestrogens and drugs. The method had a detection limit of 0.5 μmol L^{-1}, equivalent to 500 fmol.

Most POFs are composed of biocompatible light elements, such as carbon, hydrogen and nitrogen, with high biocompatibility and high stability, which make POF membranes to be a desirable candidate for biomedical fields. The use of POF membranes for biomedical applications is still in its infancy and needs to be further investigated.

3.4 Sensors

POFs have engineered and tunable building blocks at the molecular level which make them an important candidate in

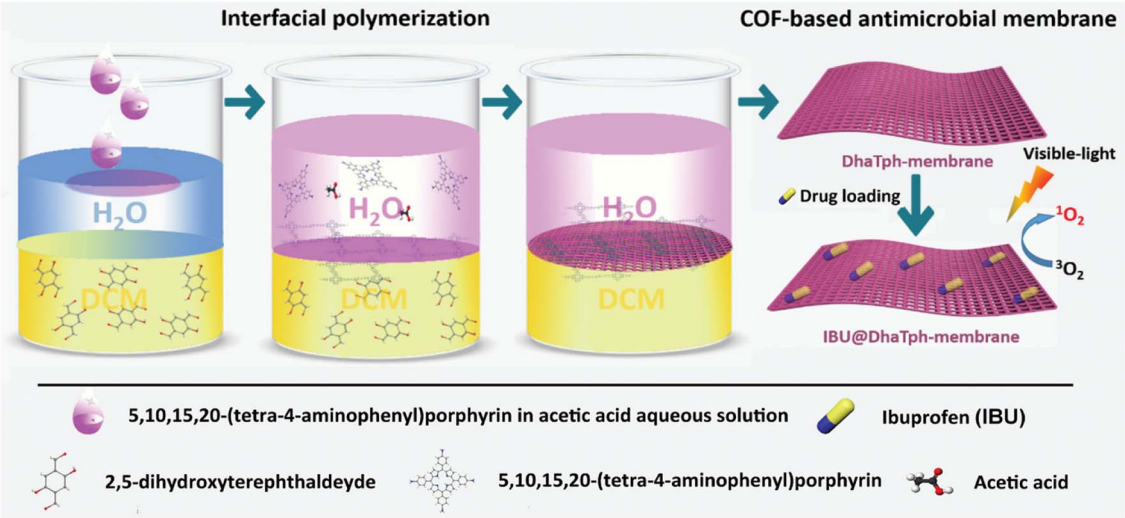

Fig. 9 Schematic illustration of the synthesis of multifunctional antimicrobial IBU@DhaTph-membrane. Copyright 2021 Wiley-VCH GmbH.

Open Access Article. Published on 16 oajagemánnu 2024. Downloaded on 2026-02-06 10:16:02.
This article is licensed under a Creative Commons Attribution-NonCommercial 3.0 Unported Licence.

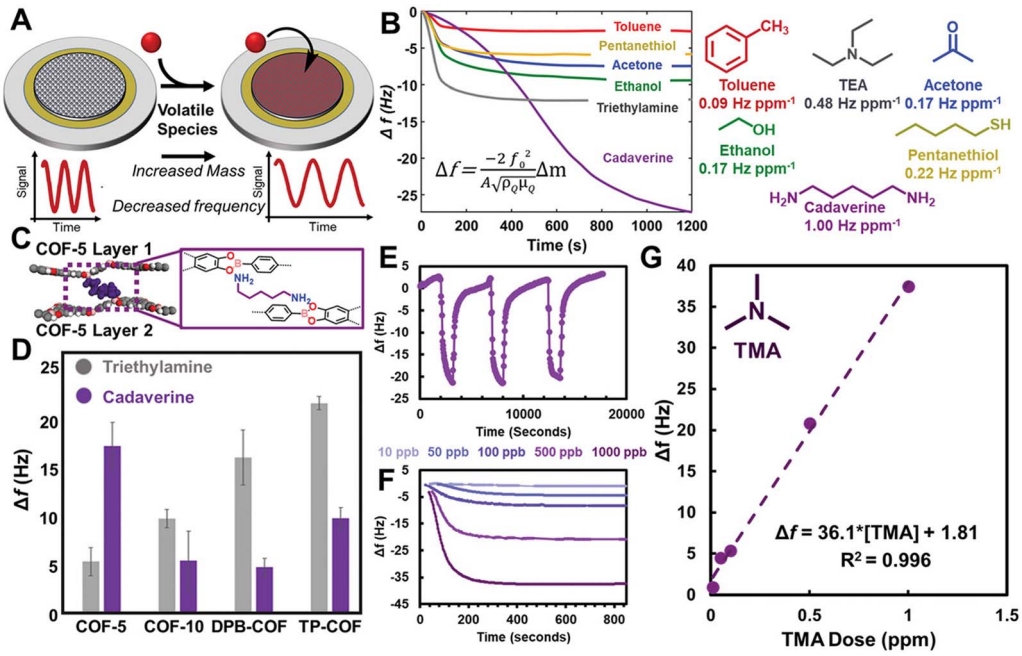

Fig. 10 (a) Schematic of the acoustic vapor sensor. (b) Frequency response of a COF-5 sensor to several volatile analytes with structures and dose-normalised responsivities shown on the right. Inset: Sauerbrey equation. (c) Computationally optimised structure of cadaverine binding between two COF-5 layers. (d) Amine responsivity of the four COFs studied. (e) Recyclability of TP-COF dosed with 500 ppb TMA, with N_2 purging between doses. (f) Dose-dependent frequency response of a TP-COF sensor to TMA. (g) TP-COF sensor calibration curve for TMA dose–response with the extracted concentration–frequency relationship. Copyright 2020 Wiley-VCH GmbH.

the field of sensing. A POF membrane constructed through an interface can be combined with its functional groups to study the sensing analysis in multiple fields such as gases, organic solvents, temperature, sound, *etc.*, which is of great significance in the fields of medical detection, information security, environmental monitoring, chemical production and so on.

In 2020, Dichtel *et al.* deposited large 2D COF films on a variety of substrate surfaces. As shown in Fig. 10, boronate-ester-linked 2D COFs had abundant porosity as well as Lewis acidity for extreme sensitivity to polar compounds, and the 2D COFs sensor showed a limit of quantification of 10 ppb for volatile trimethylamine (TMA).[99] 3D MOF thin films (Cu-HHTP) were controllably prepared using the LBL strategy by Xu *et al.* The MOF film had a high specific surface area, efficient charge transfer, and excellent sensing performance. Compared with 2D films, 3D Cu-HHTP films had 1000-fold optimised limit of detection, improved response (when the NH_3 concentration is 1 ppm) and could detect a concentration of 5 ppb of NH_3.[100] In order to expand the abundance of POF materials and improve the brittleness, Zhang's group firstly utilised interfacial polymerisation to combine polymer chains and crystalline materials to construct crystalline crosslinked polymer (CCP) membranes. The unique structure allowed the CCP membranes to exhibit good flexibility and achieve a reversible mechanical response under steam drive.[101] Ma and Sun *et al.* made some progress in the field of temperature sensing. They used acid-catalysed interfacial polymerisation to create an ionic COF membrane, which could intelligently monitor temperature changes. The sub-nanochannels could simulate thermally responsive ion channels observed in nature. The system also had the advantage of wide operating temperature, simultaneous response to temperature stimuli, and long-term stability. The potential of COF membranes in designing wearable devices with thermal sensing capability was also explored.[102,103]

Humidity levels in human metabolism contain a wealth of information. A range of humidity-sensing COF films have been developed as well.[104] Yang *et al.* synthesised COF films based on imine-bonded linkages in the water/oil interface and applied them as resistive humidity sensors. By tuning the structural monomers and functional groups, the COF films achieved the sensing performance with high response, wide detection range, fast response and recovery properties. When the relative humidity was increased from 13% to 98%, the humidity response value of the COF film-based sensor was enhanced by 390 times, revealing the amplification mechanism of humidity sensing signals by the large π-conjugated topology of the COF film.[105]

Molecular monomers with special functions (*e.g.* ionic, conjugated) have been used to construct POF membranes with external stimulus-responsive activities. This monomer design can endow POFs with new functions, which can lead to potential applications. However, the study of the chemoresistive sensing mechanism of POF materials is still in the early stage.

4 Conclusion and perspectives

We have reviewed representative novel work on the growth of porous organic membranes at interfaces in the last few years. However, due to the broad applicability of interface engineering strategies across multiple research areas, some articles may

 © 2024 The Author(s). Published by the Royal Society of Chemistry

Open Access Article. Published on 16 oajagemánnu 2024. Downloaded on 2026-02-06 10:16:02.
This article is licensed under a Creative Commons Attribution-NonCommercial 3.0 Unported Licence.

have been unintentionally overlooked in our perspective. It is exciting to see the rapid growth of this field, with numerous surface and interfacial approaches already being widely and rationally employed by the scientific community. We anticipate even greater vigour and momentum in this field in the coming years.

The structural designability and diversity of POF materials have prompted researchers to explore the versatility of POF membranes. As demonstrated in the above applications, the interface engineering strategy has penetrated into many cutting-edge application areas. Although a wide range of applications have been explored through interface engineering strategies in areas such as separation science, ion transport, and biosensing, research in molecular recognition, fluorescence imaging, and magnetism is still in its infancy. Despite substantial progress in the field of shaping POF membranes using interface technology, there are still many challenges that need to be addressed in the future. (1) Compared with the body powder, the membrane structure of POFs often has additional excellent properties, but in many cases, the continuity of the membranes obtained in this way is poor, and it is difficult to form membranes of many POF materials. (2) The excellent mechanical properties are conducive to the long-term stability of POF membranes in the industry. Nevertheless, it is difficult to guarantee the mechanical strength of the obtained membrane in most cases, and the mechanical strength is poor, which needs to be seriously considered in the future development. (3) Currently, almost all of POF thin membranes are prepared in the laboratory, so the large-scale production of POF membranes by using the interface technology and the reduction of the production cost are also the concerns of the future researchers. (4) The preparation of POF membranes with controllable orientation is challenging, which is necessary for an in-depth study of the intrinsic properties of POF membranes. So far, researchers have reported the control of the horizontal orientation of POF membranes, but the controllability of their orientation in the vertical direction has been a tough problem. (5) In applications such as ion conduction, energy storage, *etc.*, the development of POF membranes with electronic conductivity has been a focus of interest. However, only a few porous organic membranes with conductivity have been developed. Strategies such as elaborate structural design, introduction of functional groups on the backbone or composite with conductive materials will be the focus of future research.

Looking into the future, opportunities exist and the challenges are severe. We believe that the preparation of advanced porous organic materials using interface strategies will make new breakthroughs in more research areas. Time-saving, easy-to-operate, large-scale and green interface technology will be an ideal solution for membrane science and technology.

Author contributions

N. Z. and G. Z. conceived and directed this work. L. L. and R. Y. wrote the manuscript. L. Y. revised the manuscript and offered suggestions.

Conflicts of interest

There are no conflicts to declare.

Acknowledgements

We are grateful for financial support from the National Natural Science Foundation of China (Grant No. 51973026) and the Department of Science and Technology of Jilin Province (Grant No. YDZJ202201ZYTS592).

Notes and references

1 A. Thomas, *Nat. Commun.*, 2020, **11**, 4985.
2 T. Wang, R. Pan, M. L. Martins, J. Cui, Z. Huang, B. P. Thapaliya, C.-L. Do-Thanh, M. Zhou, J. Fan, Z. Yang, M. Chi, T. Kobayashi, J. Wu, E. Mamontov and S. Dai, *Nat. Commun.*, 2023, **14**, 4607.
3 H. Zhang, G. Li, J. Zhang, D. Zhang, Z. Chen, X. Liu, P. Guo, Y. Zhu, C. Chen, L. Liu, X. Guo and Y. Han, *Science*, 2023, **380**, 633–638.
4 S. Zhang, Q. Yang, C. Wang, X. Luo, J. Kim, Z. Wang and Y. Yamauchi, *Adv. Sci.*, 2018, **5**, 1801116.
5 L. Jiang, J. Jia, Y. Ma, Y. Tian, X. Zou and G. Zhu, *Chem*, 2024, **10**, 1–10.
6 S. Kandambeth, K. Dey and R. Banerjee, *J. Am. Chem. Soc.*, 2019, **141**, 1807–1822.
7 S.-Y. Yu, J. Mahmood, H.-J. Noh, J.-M. Seo, S.-M. Jung, S.-H. Shin, Y.-K. Im, I.-Y. Jeon and J.-B. Baek, *Angew. Chem., Int. Ed.*, 2018, **57**, 8438–8442.
8 Y. Tian and G. Zhu, *Chem. Rev.*, 2020, **120**, 8934–8986.
9 Q. Hao, Y. Tao, X. Ding, Y. Yang, J. Feng, R.-L. Wang, X.-M. Chen, G.-L. Chen, X. Li, H. O. Yang, X. Hu, J. Tian, B.-H. Han, G. Zhu, W. Wang, F. Zhang, B. Tan, Z.-T. Li, D. Wang and L.-J. Wan, *Sci. China: Chem.*, 2023, **66**, 620–682.
10 K. S. Song, P. W. Fritz and A. Coskun, *Chem. Soc. Rev.*, 2022, **51**, 9831–9852.
11 Y. Jing, C. Wang, Y. Chen, L. Liu, L. Yin, F. Cui, N. Zhang, S. Wen and G. Zhu, *Angew. Chem., Int. Ed.*, 2023, **62**, e202301234.
12 L. Yin, Z. Wang, Q. Wu, L. Liu, N. Zhang, Z. Xie and G. Zhu, *ACS Nano*, 2022, **16**, 6197–6205.
13 Z. Li, T. He, Y. Gong and D. Jiang, *Acc. Chem. Res.*, 2020, **53**, 1672–1685.
14 S. Yuan, X. Li, J. Zhu, G. Zhang, P. Van Puyvelde and B. Van der Bruggen, *Chem. Soc. Rev.*, 2019, **48**, 2665–2681.
15 C. Yu, X. Cen, Z. Zhang, Y. Sun, W. Xue, Z. Qiao, M. D. Guiver and C. Zhong, *Adv. Mater.*, 2023, **35**, 2307013.
16 R. Dong, T. Zhang and X. Feng, *Chem. Rev.*, 2018, **118**, 6189–6235.
17 Z. Cheng, P. Zhang, Z. Wang, H. Jiang, W. Wang, D. Liu, L. Wang, G. Zhu and X. Zou, *Small*, 2023, **19**, 2300438.
18 P. Zhang, C. Zhang, L. Wang, J. Dong, D. Gai, W. Wang, T. S. Nguyen, C. T. Yavuz, X. Zou and G. Zhu, *Adv. Funct. Mater.*, 2023, **33**, 2210091.

Open Access Article. Published on 16 oajagemánnu 2024. Downloaded on 2026-02-06 10:16:02.
This article is licensed under a Creative Commons Attribution-NonCommercial 3.0 Unported Licence.

19 T. Huang, H. Jiang, J. C. Douglin, Y. Chen, S. Yin, J. Zhang, X. Deng, H. Wu, Y. Yin, D. R. Dekel, M. D. Guiver and Z. Jiang, *Angew. Chem., Int. Ed.*, 2022, e202209306.
20 C. Zhang, B.-H. Wu, M.-Q. Ma, Z. Wang and Z.-K. Xu, *Chem. Soc. Rev.*, 2019, **48**, 3811.
21 J. Wang, H. Zhu and S. Zhu, *Chem. Eng. J.*, 2023, **466**, 143106.
22 L. Duan, C. Wang, W. Zhang, B. Ma, Y. Deng, W. Li and D. Zhao, *Chem. Rev.*, 2021, **121**, 14349–14429.
23 D. W. Burke, Z. Jiang, A. G. Livingston and W. R. Dichtel, *Adv. Mater.*, 2023, DOI: 10.1002/adma.202300525.
24 Y. Song, C. Zhu and S. Ma, *EnergyChem*, 2022, **4**, 100079.
25 N. A. Khan, R. Zhang, H. Wu, J. Shen, J. Yuan, C. Fan, L. Cao, M. A. Olson and Z. Jiang, *J. Am. Chem. Soc.*, 2020, **142**, 13450–13458.
26 M. Tu, D. E. Kravchenko, B. Xia, V. R. Giménez, N. Wauteraerts, R. Verbeke, I. F. J. Vankelecom, T. Stassin, W. Egger, M. Dickmann, H. Amenitsch and R. Ameloot, *Angew. Chem., Int. Ed.*, 2021, **60**, 7553–7558.
27 C. Lu, Y. Mo, Y. Hong, T. Chen, Z. Yang, L. Wan and D. Wang, *J. Am. Chem. Soc.*, 2020, **142**, 14350–14356.
28 X. Liu, C. Guan, S. Ding, W. Wang, H. Yan, D. Wang and L. Wan, *J. Am. Chem. Soc.*, 2013, **135**, 10470–10474.
29 Z. A. Enderson, H. Murali, R. R. Dasari, Q. Dai, H. Li, T. C. Parker, J. Brédas, S. R. Marder and P. N. First, *ACS Nano*, 2023, **17**, 7366–7376.
30 K. Sun, O. J. Silveira, Y. Ma, Y. Hasegawa, M. Matsumoto, S. Kera, O. Krejčí, A. S. Foster and S. Kawai, *Nat. Chem.*, 2023, **15**, 136–142.
31 B. Reif, J. Somboonvong, F. Fabisch, M. Kaspereit, M. Hartmann and W. Schwieger, *Microporous Mesoporous Mater.*, 2019, **276**, 29–40.
32 R. Makiura, S. Motoyama, Y. Umemura, H. Yamanaka, O. Sakata and H. Kitagawa, *Nat. Chem.*, 2010, **10**, 565–571.
33 D. B. Shinde, G. Sheng, X. Li, M. Ostwal, A.-H. Emwas, K.-W. Huang and Z. Lai, *J. Am. Chem. Soc.*, 2018, **140**, 14342–14349.
34 J. I. Feldblyum, C. H. McCreery, S. C. Andrews, T. Kurosawa, E. J. G. Santos, V. Duong, L. Fang, A. L. Ayzner and Z. Bao, *Chem. Commun.*, 2015, **51**, 13894–13897.
35 K. Liu, H. Qi, R. Dong, R. Shivhare, M. Addicoat, T. Zhang, H. Sahabudeen, T. Heine, S. Mannsfeld, U. Kaiser, Z. Zheng and X. Feng, *Nat. Chem.*, 2019, **11**, 994–1000.
36 T. Zhang, H. Qi, Z. Liao, Y. D. Horev, L. A. Panes-Ruiz, P. St. Petkov, Z. Zhang, R. Shivhare, P. Zhang, K. Liu, V. Bezugly, S. Liu, Z. Zheng, S. Mannsfeld, T. Heine, G. Cuniberti, H. Haick, E. Zschech, U. Kaiser, R. Dong and X. Feng, *Nat. Commun.*, 2019, **10**, 4225.
37 H. Sahabudeen, H. Qi, M. Ballabio, M. Položij, S. Olthof, R. Shivhare, Y. Jing, S. Park, K. Liu, T. Zhang, J. Ma, B. Rellinghaus, S. Mannsfeld, T. Heine, M. Bonn, E. Cánovas, Z. Zheng, U. Kaiser, R. Dong and X. Feng, *Angew. Chem., Int. Ed.*, 2020, **59**, 6028–6036.
38 H. Yang, Q. Sun, Z. Liao, M. Hambsch, X. Liu, D. Wu, B. Jost, Y. Zhang, S. C. B. Mannsfeld, Q. Xue, X. Feng, X. Zhu and T. Zhang, *Chem. Mater.*, 2023, **35**, 7144–7153.
39 Z. Ou, B. Liang, Z. Liang, F. Tan, X. Dong, L. Gong, P. Zhao, H. Wang, Y. Zou, Y. Xia, X. Chen, W. Liu, H. Qi, U. Kaiser and Z. Zheng, *J. Am. Chem. Soc.*, 2022, **144**, 3233–3241.
40 X. Hu, Z. Zhan, J. Zhang, I. Hussain and B. Tan, *Nat. Commun.*, 2021, **12**, 6596.
41 J. Tang, Z. Liang, H. Qin, X. Liu, B. Zhai, Z. Su, Q. Liu, H. Lei, K. Liu, C. Zhao, R. Cao and Y. Fang, *Angew. Chem., Int. Ed.*, 2023, **62**, e202214449.
42 A. O. Guerrero, H. Sahabudeen, A. Croy, A. Dianat, R. Dong, X. Feng and G. Cuniberti, *ACS Appl. Mater. Interfaces*, 2021, **13**, 26411–26420.
43 N. A. Khan, M. Luo, X. Zha, C. S. Azad, J. Lu, J. Chen, C. Fan, A. U. Rahman, M. A. Olson, Z. Jiang and D. Wang, *Small*, 2023, **19**, 2303131.
44 K. Dey, M. Pal, K. C. Rout, S. Kunjattu H, A. Das, R. Mukherjee, U. K. Kharul and R. Banerjee, *J. Am. Chem. Soc.*, 2017, **139**, 13083–13091.
45 Y. Chen, Y. Li, L. Dai, G. Qin, J. Guo, Q. Zhang, S. Li, T. A. Sherazi and S. Zhang, *Chem. Commun.*, 2021, **57**, 3131–3134.
46 M. Matsumoto, L. Valentino, G. M. Stiehl, H. B. Balch, A. R. Corcos, F. Wang, D. C. Ralph, B. J. Mariñas and W. R. Dichtel, *Chem*, 2018, **4**, 308–317.
47 Z. Zhao, M. E. EI-Khouly, Q. Che, F. Sun, B. Zhang, H. He and Y. Chen, *Angew. Chem., Int. Ed.*, 2023, **62**, e202217249.
48 R. Yang, S. Liu, Q. Sun, Q. Liao, K. Xi and B. Su, *J. Am. Chem. Soc.*, 2022, **144**, 11778–11787.
49 R. Ameloot, F. Vermoortele, W. Vanhove, M. B. J. Roeffaers, B. F. Sels and D. E. D. Vos, *Nat. Chem.*, 2011, **3**, 382–387.
50 Z. Guo, H. Wu, Y. Chen, S. Zhu, H. Jiang, S. Song, Y. Ren, Y. Wang, X. Liang, G. He, Y. Li and Z. Jiang, *Angew. Chem., Int. Ed.*, 2022, **61**, e202210466.
51 Q. Hao, C. Zhao, B. Sun, C. Lu, J. Liu, M. Liu, L.-J. Wan and D. Wang, *J. Am. Chem. Soc.*, 2018, **140**, 12152–12158.
52 J. Liu, G. Han, D. Zhao, K. Lu, J. Gao and T.-S. Chung, *Sci. Adv.*, 2020, **6**, eabb1110.
53 Z. Gao, J. Liu and T.-S. Chung, *Sep. Purif. Technol.*, 2022, **294**, 121166.
54 J. Liu, D. Hua, Y. Zhang, S. Japip and T.-S. Chung, *Adv. Mater.*, 2018, **30**, 1705933.
55 P. Shao, J. Li, F. Chen, L. Ma, Q. Li, M. Zhang, J. Zhou, A. Yin, X. Feng and B. Wang, *Angew. Chem., Int. Ed.*, 2018, **57**, 16501–16505.
56 D. Zhou, X. Tan, H. Wu, L. Tian and M. Li, *Angew. Chem., Int. Ed.*, 2019, **58**, 1376–1381.
57 A. Giri, G. Shreeraj, T. K. Dutta and A. Patra, *Angew. Chem., Int. Ed.*, 2023, **62**, e202219083.
58 Y. Ma, L. Liu, H. Lei, Y. Tian, S. Ding, N. Zhang and G. Zhu, *Inorg. Chem. Commun.*, 2022, **141**, 109526.
59 J. W. Colson, A. R. Woll, A. Mukherjee, M. P. Levendorf, E. L. Spitler, V. B. Shields, M. G. Spencer, J. Park and W. R. Dichtel, *Science*, 2011, **332**, 228–231.
60 J. Heinze, B. A. Frontana-Uribe and S. Ludwigs, *Chem. Rev.*, 2010, **110**, 4724.
61 C. Gu, Y. Chen, Z. Zhang, S. Xue, S. Sun, K. Zhang, C. Zhong, H. Zhang, Y. Pan, Y. Lv, Y. Yang, F. Li, S. Zhang, F. Huang and Y. Ma, *Adv. Mater.*, 2013, **25**, 3443–3448.

 © 2024 The Author(s). Published by the Royal Society of Chemistry

Open Access Article. Published on 16 oajagemánnu 2024. Downloaded on 2026-02-06 10:16:02.
This article is licensed under a Creative Commons Attribution-NonCommercial 3.0 Unported Licence.

62 Z. Zhou, D. B. Shinde, D. Guo, L. Cao, R. A. Nuaimi, Y. Zhang, L. R. Enakond and Z. Lai, *Adv. Funct. Mater.*, 2022, **32**, 2108672.
63 Y. Wang, S. Zhang, J. Wu, K. Liu, D. Li, Q. Men and G. Zhu, *ACS Appl. Mater. Interfaces*, 2017, **9**, 43688–43695.
64 L. Yin, L. Liu and N. Zhang, *Chem. Commun.*, 2021, **57**, 10484–10499.
65 B. Liang, H. Wang, X. Shi, B. Shen, X. He, Z. A. Ghazi, N. A. Khan, H. Sin, A. M. Khattak, L. Li and Z. Tang, *Nat. Chem.*, 2018, **10**, 961–967.
66 L. Liu, L. Yin, D. Cheng, S. Zhao, H. Zang, N. Zhang and G. Zhu, *Angew. Chem., Int. Ed.*, 2021, **60**, 14875–14880.
67 L. Liu, Y. Ma, B. Li, L. Yin, H.-Y. Zang, N. Zhang, H. Bi, S. Wang and G. Zhu, *Small*, 2023, DOI: **10.1002/smll.202308499**.
68 R. Banerjee, A. Phan, B. Wang, C. Knobler, H. Furukawa, M. O'keeffe and O. M. Yaghi, *Science*, 2008, **319**, 939–943.
69 X. Ma, P. Kumar, N. Mittal, A. Khlyustova, P. Daoutidi, K. A. Mkhoyan and M. Tsapatsis, *Science*, 2018, **361**, 1008–1011.
70 Y. Miao, D. T. Lee, M. D. Mello, M. Ahmad, M. K. Abdel-Rahman, P. M. Eckhert, J. A. Boscoboinik, D. H. Fairbrother and M. Tsapatsis, *Nat. Commun.*, 2022, **13**, 420.
71 G. Lu and J. T. Hupp, *J. Am. Chem. Soc.*, 2010, **132**, 7832–7833.
72 Q. Liu, Y. Miao, L. F. Villalobos, S. Li, H. Chi, C. Chen, M. T. Vahdat, S. Song, D. J. Babu, J. Hao, Y. Han, M. Tsapatsis and K. V. Agrawal, *Nat. Mater.*, 2023, **22**, 1387–1393.
73 F. G. Fabozzi, N. Severin, J. P. Rabe and S. Hecht, *J. Am. Chem. Soc.*, 2023, **145**, 18205–18209.
74 P. Mocny and H. Klok, *Prog. Polym. Sci.*, 2020, **100**, 101185.
75 M. Ratsch, C. Ye, Y. Yang, A. Zhang, A. M. Evans and K. Börjesson, *J. Am. Chem. Soc.*, 2020, **142**, 6548–6553.
76 L. Hou, M. Zhou, X. Dong, L. Wang, Z. Xie, D. Dong and N. Zhang, *Chem.–Eur. J.*, 2017, **23**, 13337–13341.
77 R. Yu, L. Liu, L. Yin, Y. Jing, N. Zhang, H. Bian and G. Zhu, *Chem. Sci.*, 2023, **14**, 3782–3788.
78 Z.-A. Qiao, S.-H. Chai, K. Nelson, Z. Bi, J. Chen, S. M. Mahurin, X. Zhu and S. Dai, *Nat. Commun.*, 2014, **5**, 3705.
79 J. Wu, F. Hillman, C.-Z. Liang, Y. Jia and S. Zhang, *J. Mater. Chem. A*, 2023, **11**, 17452–17478.
80 Y. Ma, F. Cui, H. Rong, J. Song, X. Jing, Y. Tian and G. Zhu, *Angew. Chem., Int. Ed.*, 2022, **61**, e202113682.
81 B. Wang, Z. Qiao, J. Xu, J. Wang, X. Liu, S. Zhao, Z. Wang and M. D. Guiver, *Adv. Mater.*, 2020, **32**, 1907701.
82 H. Fan, A. Mundstock, A. Feldhoff, A. Knebel, J. Gu, H. Meng and J. Caro, *J. Am. Chem. Soc.*, 2018, **140**, 10094–10098.
83 H. Fan, M. Peng, I. Strauss, A. Mundstock, H. Meng and J. Caro, *Nat. Commun.*, 2021, **12**, 38.
84 H. Fan, H. Wang, M. Peng, H. Meng, A. Mundstock, A. Knebel and J. Caro, *ACS Nano*, 2023, **17**, 7584–7594.
85 Y. Ying, S. B. Peh, H. Yang, Z. Yang and D. Zhao, *Adv. Mater.*, 2022, **34**, 2104946.
86 Y. Li, Q. Wu, X. Guo, M. Zhang, B. Chen, G. Wei, X. Li, X. Li, S. Li and L. Ma, *Nat. Commun.*, 2020, **11**, 599.
87 N. A. Khan, R. Zhang, X. Wang, L. Cao, C. S. Azad, C. Fan, J. Yuan, M. Long, H. Wu, M. A. Olson and Z. Jiang, *Nat. Commun.*, 2022, **13**, 3169.
88 J. Li, H. Rong, Y. Chen, H. Zhang, T. X. Liu, Y. Yuan, X. Zou and G. Zhu, *Chem. Commun.*, 2020, **56**, 6519–6522.
89 L. Cao, I. Chen, Z. Li, X. Liu, M. Mubashir, R. A. Nuaimi and Z. Lai, *Nat. Commun.*, 2022, **13**, 7894.
90 X. Zuo, C. Zhu, W. Xian, Q. Meng, Q. Guo, X. Zhu, S. Wang, Y. Wang, S. Ma and Q. Sun, *Angew. Chem.*, 2022, **134**, e202116910.
91 L. Cao, H. Wu, P. Yang, X. He, J. Li, Y. Li, M. Xu, M. Qiu and Z. Jiang, *Adv. Funct. Mater.*, 2018, **28**, 1804944.
92 C. Fan, H. Geng, H. Wu, Q. Peng, X. Wang, B. Shi, Y. Kong, Z. Yin, Y. Liu and Z. Jiang, *J. Mater. Chem. A*, 2021, **9**, 17720–17723.
93 K. Wang, H. Yang, Z. Liao, Z. Liao, S. Li, M. Hambsch, G. Fu, S. C. B. Mannsfeld, Q. Sun and T. Zhang, *J. Am. Chem. Soc.*, 2023, **145**, 5203–5210.
94 Y. Shi, Y. Wang, J. Bi, H. Zuo, W. Long, W. Zhang and Y. Liao, *Sci. China Mater.*, 2023, **66**, 3319–3326.
95 H. R. Alanagh, I. Rostami, M. Taleb, X. Gao, Y. Zhang, A. M. Khattak, X. He, L. Li and Z. Tang, *J. Mater. Chem. B*, 2020, **8**, 7899–7903.
96 L. Ding, S. Wang, B. Yao, F. Li, Y. Li, G. Zhao and Y. Dong, *Adv. Healthcare Mater.*, 2021, **10**, 2001821.
97 X. Yan, H. Li, T. Yin, G. Jie and H. Zhou, *Biosens. Bioelectron.*, 2022, **217**, 114694.
98 Z. Chen, Y. Wu, D. Ouyang and Z. Lin, *Rapid Commun. Mass Spectrom.*, 2023, **37**, e9463.
99 A. M. Evans, N. P. Bradshaw, B. Litchfield, M. J. Strauss, B. Seckman, M. R. Ryder, I. Castano, C. Gilmore, N. C. Gianneschi, C. R. Mulzer, M. C. Hersam and W. R. Dichtel, *Adv. Mater.*, 2020, **32**, 2004205.
100 Y. Lin, W. Li, Y. Wen, G. Wang, X. Ye and G. Xu, *Angew. Chem., Int. Ed.*, 2021, **60**, 25758–25761.
101 E. Lin, Z. Wang, X. Zhao, Z. Liu, D. Yan, F. Jin, Y. Chen, P. Cheng and Z. Zhang, *Angew. Chem., Int. Ed.*, 2022, **61**, e202117390.
102 P. Zhang, S. Chen, C. Zhu, L. Hou, W. Xian, X. Zuo, Q. Zhang, L. Zhang, S. Ma and Q. Sun, *Nat. Commun.*, 2021, **12**, 1844.
103 W. Xian, P. Zhang, C. Zhu, X. Zuo, S. Ma and Q. Sun, *CCS Chem.*, 2021, **3**, 2464–2472.
104 A. Mei, W. Chen, Z. Yang, M. Zhou, W. Jin, S. Yang, K. Chen and Y. Liu, *Angew. Chem., Int. Ed.*, 2023, **62**, e202301440.
105 X. Chen, L. Kong, J. A. Mehrez, C. Fan, W. Quan, Y. Zhang, M. Zeng, J. Yang, N. Hu, Y. Su, H. Wei and Z. Yang, *Nano-Micro Lett.*, 2023, **15**, 149.